

Corrosion inhibition of low carbon steel in CO₂ -saturated solution using Anionic surfactant

Hany M. Abd El-Lateef^{*1,2}, L. I. Aliyeva¹, V. M. Abbasov¹, T. I. Ismayilov¹

¹*Mamedaliev Institute of Petrochemical Processes, National Academy of Sciences of Azerbaijan, AZ1025 Baku, Azerbaijan*

²*Chemistry Department, Faculty of Science, Sohag University, Sohag, Egypt*

ABSTRACT

Corrosion inhibition of carbon steel alloy in 1.0 % NaCl saturated with CO₂ by synthesized sulfated fatty acid sodium salt (SFASS) as an anionic surfactant inhibitor have been investigated using weight loss measurements, Extrapolation of cathodic and anodic Tafel plot and Linear Polarization Resistance (LPR bubble test). The data obtained from all the used methods are in good agreement with each other. These studies have shown that SFASS is a very good "green", mixed-type inhibitor. The inhibition process was attributed to the formation of an adsorbed film on the metal surface that protects the metal against corrosive agents. The inhibition efficiency increases with increasing both the concentration of the studied inhibitor and temperature. Maximum inhibition efficiency of the surfactant is observed at concentrations around its critical micellar concentration (CMC). The surface activity of the synthesized surfactant solutions was determined using surface and interfacial tension measurements at 25 °C. Thermodynamic adsorption parameters of studied inhibitor were calculated using the Langmuir adsorption isotherm. The protective film formation on metal surface is investigated by means of FTIR.

Keywords: Corrosion inhibition, Carbon steel, Surfactant, LPR bubble test, SFASS, FTIR.

INTRODUCTION

Carbon steel is used in mass amounts in marine applications, chemical processing, petroleum production and refining, construction and metal-processing equipment [1–3], despite it has a relatively high cost. These applications usually induce serious corrosive effect on equipments, tubes and pipelines made of iron and its alloys [4].

Carbon dioxide (CO₂) corrosion is one of the major problems in oil and gas industry, costing billions of dollars every year [5]. In CO₂ corrosion, CO₂ dissolves and hydrates to form carbonic acid (H₂CO₃), which then dissociates into bicarbonate, carbonate and hydrogen ions [6–11]. Due to its low cost and availability, carbon steel is used as the primary construction material for pipelines in oil and gas industries, but it is very susceptible to corrosion in CO₂ environments. Aqueous carbon dioxide (carbonic acid) is corrosive and corrodes the carbon steel pipelines. Carbon dioxide corrosion has been of interest to researchers in oil industries for many years and there exists many theories about the mechanism of CO₂ corrosion [12, 13]

The mechanisms of CO₂ corrosion and the formation and removal of protective iron carbonate films are not fully understood due to the complex reaction mechanisms and the presence of many critical environmental factors such as pH, temperature, dissolved species concentration and hydrodynamics that can appreciably change the corrosion rate.

In addition, CO₂ corrosion products can also form protective iron carbonate (FeCO₃) films on the surface under certain conditions and can prevent the metal from further corrosion by acting as a diffusion barrier [14]. The protective nature of these iron carbonate films depends on the environmental factors as well. Understanding the properties of surface films and the rate at which they form on the pipelines due to the presence of carbon dioxide will help in achieving better protection of oil tube steels. It will also help to increase the efficacy of corrosion mitigation techniques.

The application of inhibitors to prevent corrosion of metals is an extremely important area of concern [15]. The inhibition mechanisms are (i) the inhibitor is adsorbed on the surface of the metal forming a compact protective thin layer, and (ii) the inhibitor forms a precipitate on the surface of the metal, acting on the aggressive medium to form protective precipitates or remove aggressive agents. Some inhibitors act on the cathode (cathodic inhibitor) or on the anode (anodic inhibitor) or on both (mixed mechanism inhibitor) [15–17].

Specific types of organic inhibitors are represented by surfactants [18–28]. Surfactant molecules consist of nonpolar hydrophobic and polar hydrophilic groups. In the general case, the inhibitive effect of surfactants is due to their adsorption at the metal [29]. The adsorption of a surfactant from its solution at a metal or oxide is always a complex process involving displacement of organic molecules from the bulk of the solution to the interface (hydrophobic effect), desorption of solvent molecules from the metal or its oxide, and finally the formation of a bond between a surfactant molecule and the surface.

This article reports the use of weight loss, Extrapolation of cathodic and anodic Tafel plot and Linear Polarization Resistance (LPR bubble test) with IR observations to study the ability of sulfated fatty acid sodium salt as an anionic surfactant synthesized based on sunflower oil (Fig. 1), to inhibit the corrosion of low carbon steel in 1.0% NaCl solution saturated with CO₂ under the influence of various experimental conditions. It was also the purpose of the present work to test the experimental data obtained from the three techniques with several adsorption isotherms at different temperatures, in order to determine the thermodynamic functions for the adsorption process and gain more information on the mode of adsorption. The protective film formation on metal surface is investigated by means of FTIR

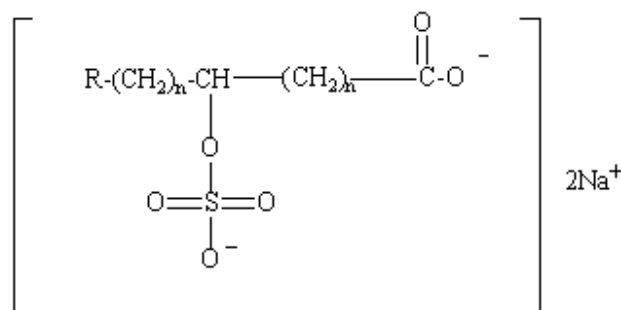


Fig. 1: Molecular structure of the synthesized anionic surfactant (SFAS).

MATERIALS AND METHODS

2.1. Chemical composition of carbon steel alloy

Electrodes are made of carbon steel grade 080A15 and have an area of 7.9 cm². The mechanical properties of the carbon steel measured at room temperature were provided by supplier shown as follows: tensile strength equal to 490 MPa and elongation to failure equal to 16%. The Chemical composition of low carbon steel used in this study was given in Table 1. The data was provided by European Corrosion Supplies Ltd.

Table 1: Chemical composition of low carbon steel

Element	Si	Ni	Cr	C	S	P	Mn	Fe
Content, (wt. %)	0.24	0.01	0.10	0.18	0.05	0.05	0.50	Balance

2.2. Synthesis of the inhibitors

Sunflower oil was heated with an alkali at a temperature of 90-95 °C, then mix in the interaction of hydrochloric acid, formed two layers. Acid formed in the upper layer was collected. The resulting acid was separated and washed with hot water. The physical and chemical properties of acid was studied and given in Table 2.

Fatty acids which produced from oil were used as base materials for sulfating process. The sulfating process was done in a 500 ml ground glass three-neck flask equipped with a mechanical stirrer, a thermometer with a temperature controller, were charged with 100 gm fatty acid and then 30 ml 10% sulfuric acid (Sulfating agent) was added drop by drop at the reaction temperature in the range from 70 to 75 °C with stirring for 7 h. The product is Sulfated fatty acid (Acid number = 280 mg KOH/g, pH=4.8). The chemical structure of the synthesized compound was confirmed by FTIR spectroscopy in the range 4000–500 cm^{-1} . Sulfated fatty acid was treated in the equimolar ratio with 25% NaOH, at room temperature to produce a sodium salt. The chemical structure of the synthesized surfactant was characterized by physical-chemical spectroscopic methods.

Table 2: Physical and chemical properties of fatty acid obtained from sunflower oil.

Acid number mg KOH/g	Molecular weight g/mol	Iodine number 100 g iodine / g of sample	Density D_4^{20} kg/m^3	Refraction, η_{20}^D
145.6	279	112	907.5	1.4680

2.3. Corrosion inhibition test

The aggressive solution, 1 % NaCl, was prepared by dissolving of analytical grade NaCl in distilled water. The concentration range of the prepared surfactant was from 10 to 100 ppm used for corrosion measurements. All solutions were prepared using a mixture from distilled water and isopropyl alcohol in a ratio 70:30.

2.4. Corrosion measurements

The measurements were performed on the cylinder electrode ($A=7.9 \text{ cm}^2$). This electrode was using for one time. Prior to each measurement the electrodes were degreased in pure acetone and washed in running bidistilled water before being inserted in the polarization cell. The reference electrode was a saturated calomel electrode (SCE) to which all potentials are referred.

The cell description is given elsewhere [30]. Before begin experiment, the prepared 1% - of the solution sodium chloride was stirred by a magnetic stirrer for 30 min in 1000 ml cell. Then this cell was placed on a heater at a temperature range 20 -50 °C for 1 hour under a pressure of 0.9 bars. The solution was saturated with carbon dioxide. To remove any surface contamination and air formed oxide, the working electrode was kept at -1500 mV (SCE) for 5 min in the tested solution, disconnected shaken free of adsorbed hydrogen bubbles and then cathodic and anodic polarization was recorded. ACM GILL AC instrument connected with a personal computer was used for the measurements.

Each experiment was performed with freshly prepared solution and clean set of electrodes. Measurements were conducted at temperature range 20-50 °C for the investigated NaCl solution. For this purpose, Magnetic Stirrer with Heater (115 V, 50/60 Hz) was used.

The extrapolation of cathodic and anodic Tafel lines was carried out in a potential range $\pm 200 \text{ mV}$ with respect to corrosion potential (E_{corr}) at scan rate of 1 mV s^{-1} ,

Linear polarization studies were made using a “LPR bubble test” method. The LPR method is ideal for plant monitoring offering an almost instantaneous indication of corrosion rate, allowing for quick evaluation of remedial action and minimizing unscheduled downtime. The potential of the working electrode was varied by a CoreRunning programme (Version 5.1.3.) through an ACM instrument Gill AC. The CoreRunning programme converts a corrosion current in mA/cm^2 to a corrosion rate in mm/year . As a working electrode was used, a cylindrical carbon steel rod of the composition 080A15GRADE STEEL. An exposed area of electrode is 7.19 cm^2 . This electrode is for disposable using and keeping in inhibitor. Gill AC technology allows measure DC and AC signals using standard Sequencer software. A small sweep from typically -10 mV to $+10 \text{ mV}$ at 10 mV/min around the rest potential is performed.

For weight loss measurements, corrosion inhibition tests were performed using cylindrical rods 7.19 cm³. These cylindrical rods were washed with deionized water, degreased with absolute ethanol. The cylindrical rods were dried and kept in a desiccator. The weight loss (in mg/cm²) was determined at different immersion times by weighing the cleaned samples before and after hanging the cylindrical rods into 1000 cm³ of the corrosive solution, namely 1% NaCl saturated with CO₂ in closed beaker in the absence and presence of various concentrations of investigated surfactant.

2.5. Surface tension measurements

It is of interest to study the micellar properties of solutions of these compounds in order to correlate their surface active properties with critical micelle concentration (CMC). The Sodium salt of Sulfated fatty acid is interesting example of surfactants with two hydrophilic groups. The surface tension (γ) was measured using (DuNouy Tensiometer, Kruss Type 8451) for various concentrations of the investigated surfactant.

2.6. Surface examination by FTIR analysis

The carbon steel specimens were immersed in solutions with inhibitor for four days. After that, the specimens were taken out and dried. The nature of the film formed on the surface of the metal specimens was analyzed by FTIR. These spectra were recorded by FTIR spectroscopy in the range 4000–500 cm⁻¹.

FTIR spectra were recorded in a Perkins – Elmer 1600 spectrophotometer. The film was carefully removed, mixed thoroughly with KBr made into pellets and FTIR spectra were recorded.

RESULTS AND DISCUSSION

3.1. Weight loss measurements

Figure 2 shows the variation of the weight loss (in mg/cm²) of carbon steel with the immersion time in 1% NaCl solution saturated with CO₂ in the absence and presence of various concentrations (10-100 ppm) of SFASS at 50 °C. It is obvious from Figure 2 that, the weight loss decreased, and therefore the corrosion inhibition strengthened, with increase in inhibitor concentration. This trend may result from the fact that adsorption and surface coverage increases with the increase in concentration; thus the surface is efficiently separated from the medium [31].

As the results the surface coverage (θ) of compounds is increasing more clearly. This surface coverage (θ) is calculated using the following equation:

$$\theta = \frac{W_0 - W}{W_0} \quad (1)$$

Where W_0 and W are the weight losses per unit area in the absence and presence of the inhibitor, respectively. The percentage inhibition efficiency, (IE %), of the surfactants is calculated by applying the following equation [32-33] :

$$IE, \% = \frac{W_0 - W}{W_0} \times 100 \quad (2)$$

The effect of the inhibitor concentration on the corrosion rate was examined; detailed experimental results were collected in Table 3 and graphically represented in Fig. 3. At a given temperature, the inhibition efficiency increases with increasing SFASS concentration, and the highest inhibition efficiencies are observed when the SFASS concentration reaches values close to its critical micellar concentration (CMC). As the concentration of surfactant molecules approaches the CMC, micelles form in solution, and similar aggregate structures such as bilayers and multilayers form on the surface (see Figure 4). Further increase in surfactant concentration above the CMC results in other types of aggregates such as lamellar structures and rod-like micelles that can form in solution as well as analogous bilayers or multilayers that form at interfaces [34, 35].

Consequently, in the context of corrosion inhibition using surfactants, the CMC marks an effective boundary condition below which surfactant adsorption is typically below the monolayer level, and above which adsorption can

consist of multiple layers of adsorbed surfactant molecules. Above the CMC, increasing surfactant concentration leads to the gradual formation of multilayers that further reduce the rate of corrosion.

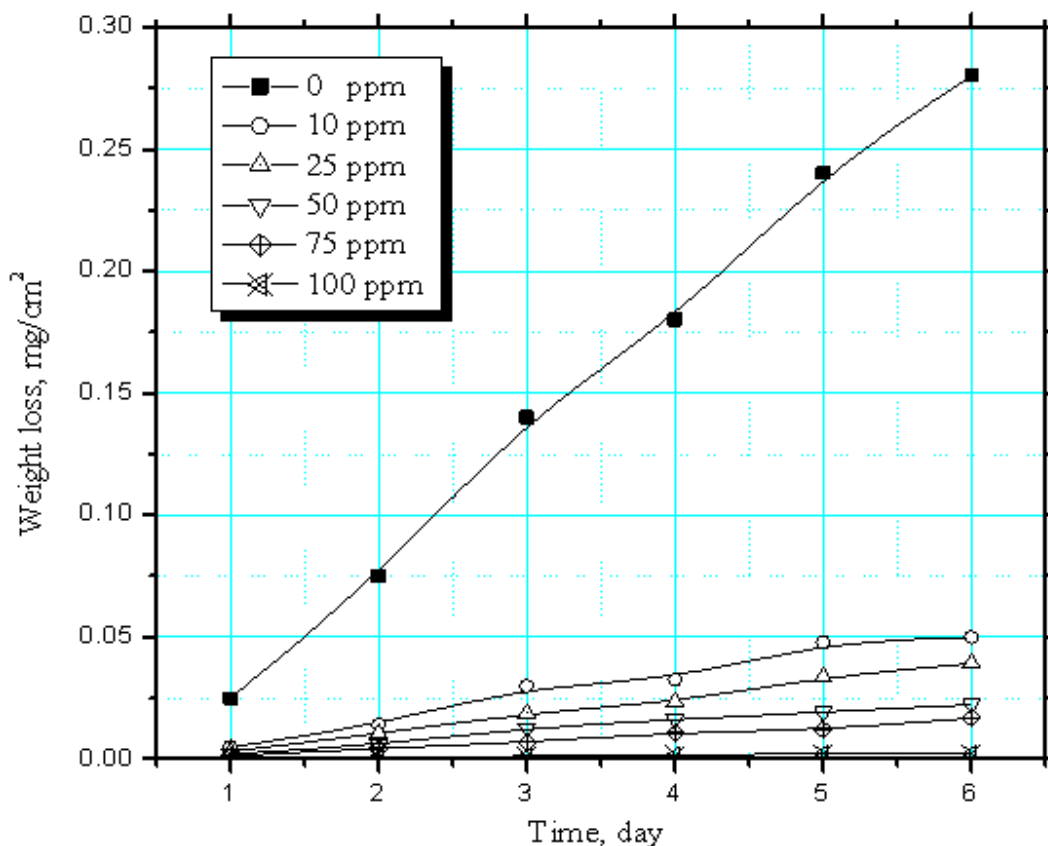


Fig. 2. Weight loss–time curves of carbon steel in 1%NaCl solution saturated with CO₂ in the absence and presence of different concentrations of SFASS inhibitor.

Table 3: Dependence of the corrosion rate of carbon steel, the degree of surface coverage (θ) and the percentage inhibition efficiency ($IE\%$) on the concentration of the synthesized inhibitor (SFASS) at 50 °C

Concentration, ppm	Corrosion rate (mg cm ⁻² per day)	θ	$IE\%$
0	0.1566	---	---
10	0.0299	0.8090	80.90
25	0.0215	0.8627	86.27
50	0.0131	0.9163	91.63
75	0.0087	0.9444	94.44
100	0.0013	0.9916	99.16

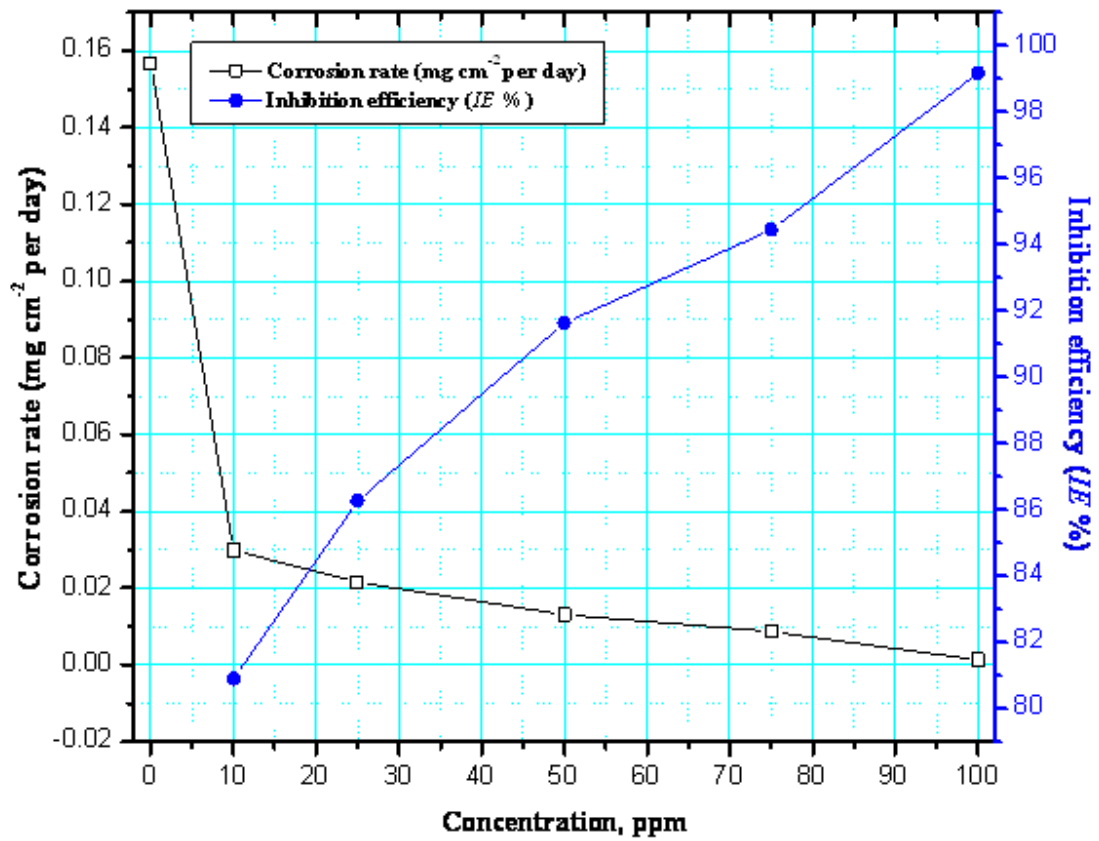


Fig. 3. Variation of the corrosion rate and inhibition efficiency with the concentration of the inhibitor in ppm at 50 °C.

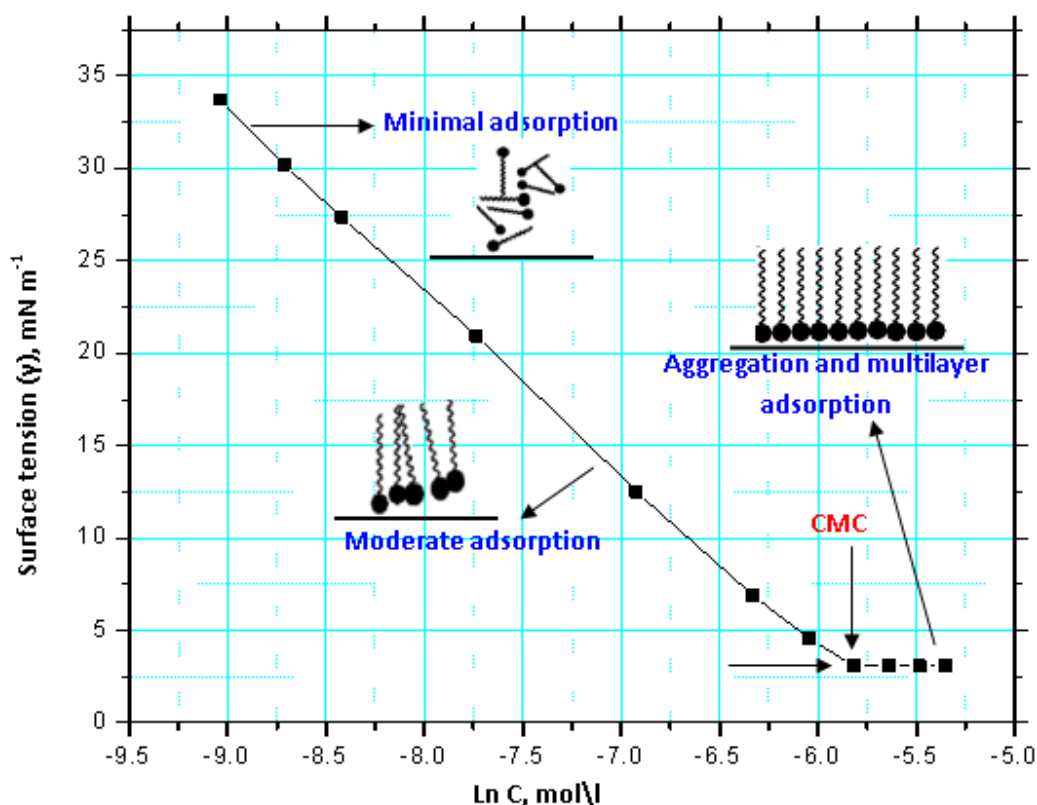


Fig. 4: Change of surface tension (γ) with the concentration of the synthesized inhibitor at 298 K.

3.2. Extrapolation of cathodic and anodic Tafel lines

Steady state of open circuit corrosion potential (E_{corr}) for the investigated electrode in the absence and presence of the studied inhibitor was attained after 45–60 min from the moment of immersion. Corrosion current density (I_{corr}) of the investigated electrode was determined [36]. By extrapolation of cathodic and anodic Tafel lines to corrosion potential (E_{corr}). The inhibition efficiency expressed as percent inhibition ($IE\%$) is defined as

$$IE\% = \frac{I_{\text{uninh.}} - I_{\text{inh.}}}{I_{\text{uninh.}}} \times 100 \quad (3)$$

Where $I_{\text{uninh.}}$ and $I_{\text{inh.}}$ are the uninhibited and inhibited corrosion currents. The inhibited corrosion currents are those determined in the presence of the studied surfactant used in this investigation. The uninhibited corrosion currents were determined in pure (inhibitor free) 1% NaCl saturated with CO_2 at the same temperature.

Figure 5 show the influence of SFASS concentrations on the Tafel cathodic and anodic polarization characteristics of low carbon steel in 1.0% NaCl solution saturated with CO_2 of scan rate 1 mV s^{-1} and at 50°C . Corrosion parameters were calculated on the basis of cathodic and anodic potential versus current density characteristics in the Tafel potential region [37, 38]. It can be seen that the presence of surfactant molecule results a marked shift in both cathodic and anodic branches of the polarization curves towards lower current densities. This means that, the

inhibitor affects both cathodic and anodic reactions. It was found that, both anodic and cathodic reactions of carbon steel electrode corrosion were inhibited with increasing concentration of synthesized inhibitor. These results suggest that not only the addition of synthesized inhibitor reduce anodic dissolution but also retard the hydrogen evolution reaction. The results showed that the inhibiting action of this inhibitor on the both cathodic and anodic processes seems to approximately be equal. The inhibitor may decrease the corrosion through the reduction of carbon steel reactivity. Accordingly to this mechanism, a reduction of either the anodic or the cathodic reaction or both arises from the adsorption of the inhibitor on the corresponding active sites [39].

The data in Table 3 exhibited that the corrosion current density (I_{corr}) decreases, and the inhibition efficiency ($IE\%$) increases as the concentration of SFASS is increased. These results suggest that retardation of the electrodes processes occurs, at both cathodic and anodic sites, as a result of coverage of these sites by surfactant molecule. The increase of inhibitor efficiency with increasing the concentration can be interpreted on the basis the adsorption amount and the coverage of surfactants molecules, increases with increasing concentration [40]. The E_{corr} value of the synthesized inhibitor was shifted slightly toward both cathodic and anodic directions and did not show any definite trend. This may be contributed to the mixed-type behaviour of the studied inhibitors.

The fact that the slopes of the cathodic (β_c) and anodic (β_a) Tafel lines in Table 3 are approximately constant and independent of inhibitor concentration. These results indicate that this inhibitor act by simply blocking the available surface area. In other words, the inhibitor decreases the surface area for corrosion of the investigated metal, and only causes inactivation of a part of the surface with respect to corrosive medium [36].

The high θ value (see Table 3) near unity indicates almost a full coverage of the metal surface with adsorbed surfactant molecule. Conclusively, the surfactant inhibitor having θ near unity is considered as a good physical barrier shielding the corroding surface from corrosive medium and dumping the corrosion rate of carbon steel significantly.

Table 4: Corrosion parameters obtained from Tafel polarization for carbon steel in 1.0% NaCl saturated with CO_2 in absence and presence of different concentrations of SFASS at 50 °C.

Conc. of inhibitor (ppm)	E_{corr} (mV(SCE))	I_{corr} (μAcm^{-2})	β_a (mVdec ⁻¹)	$-\beta_c$ (mVdec ⁻¹)	θ	$IE, \%$
0.0	-687	2100	175	124	---	---
10	-637	336	172	120	0.840	84
25	-650	254	173	121	0.879	87.9
50	-603	111	175	121	0.947	94.7
75	-562	53	174	122	0.974	97.4
100	-572	11	174	122	0.995	99.5

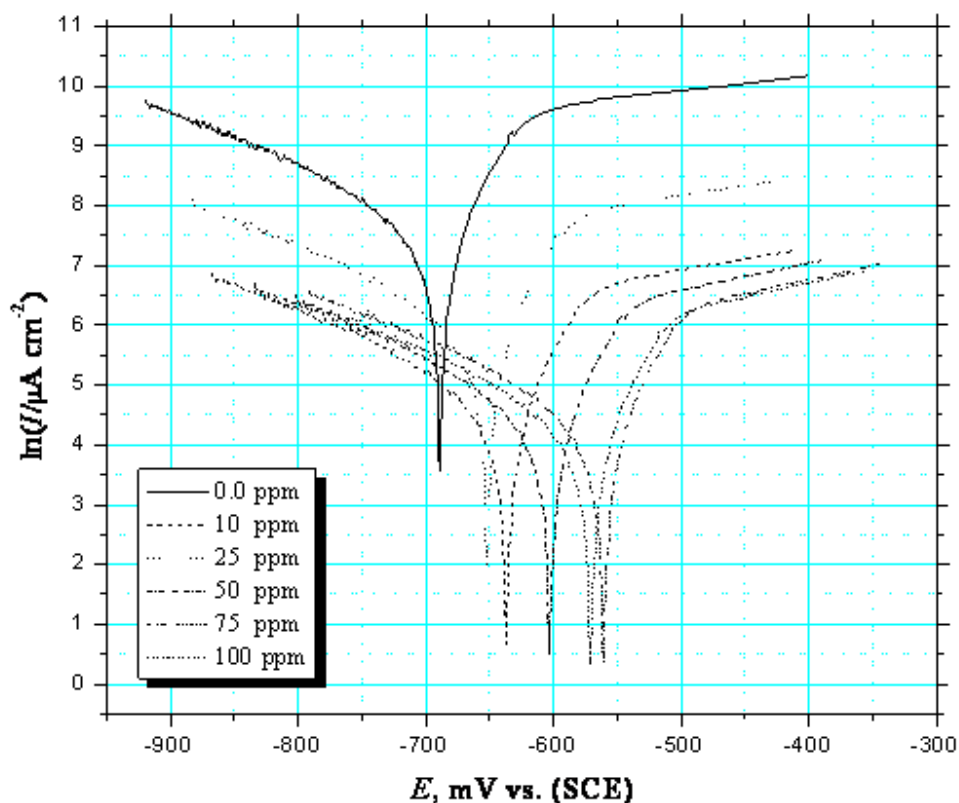


Fig. 5: Tafel polarization curves for carbon steel in 1% NaCl saturated with CO₂ containing different concentrations of SFASS at 50 °C.

3.3. Linear polarization studies (LPR bubble test)

In order to support the data obtained from those extrapolation of cathodic and anodic Tafel lines and weight loss measurements, LPR bubble test of carbon steel in 1.0% solution of NaCl saturated with CO₂ containing various concentrations of surfactant is examined. LPR bubble test has been performed in brine saturated with CO₂ at 50 °C, in turbulence fluid stream during 20 hours. Figure 6 shows the Effect of SFASS concentrations on the kinetics corrosion of carbon steel in 1% NaCl solution saturated with CO₂ at 50 °C. Corrosion parameters were calculated on the basis of LPR test. It can be seen that the presence of inhibitor results a high decrease in the rate of corrosion. This may be contributed to stable protective film which formed on the metal surface.

The data in Table 5 exhibited that the corrosion rate decreases, and the inhibition efficiency ($IE\%$) increases as the concentration of inhibitors is increased. The increase of inhibitor efficiency with increasing the concentration can be interpreted on the basis of the adsorption amount and the coverage of surfactants molecules, increases with increasing concentration.

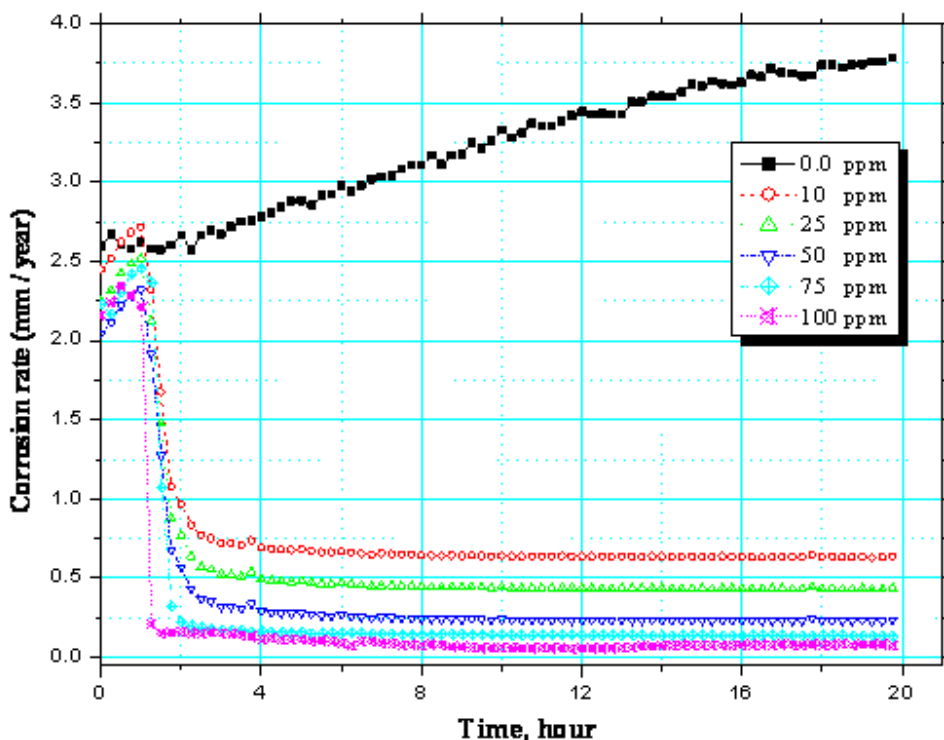


Fig. 6: Effect of SFASS concentrations on the kinetics corrosion of carbon steel in 1% NaCl solution saturated with CO₂ at 50 ° C.

Table 5: The corrosion parameters for carbon steel electrode in 1% solution of NaCl saturated with CO₂ in the absence and presence of various concentrations of SFASS at 50 ° C.

Inhibitor	Concentration, ppm	Corrosion rate (mm/year)	The inhibition efficiency, IE%
1% NaCl without inhibitor	0.0	3.78	-----
SFASS	10	0.63647	83.20
	25	0.43514	88.48
	50	0.23745	93.73
	75	0.13572	96.40
	100	0.02113	99.44

3.4. Effect of temperature

In order to gain more information about the type of adsorption and the effectiveness of the studied inhibitor at higher temperatures, cathodic and anodic Tafel polarization was performed at different temperatures (20–50 °C) for carbon steel 1.0% NaCl solution saturated with CO₂ without and with selected concentrations of the studied inhibitor. The data exhibit that the inhibition efficiency increases with increasing temperature in the presence of inhibitor (Fig. 7). This behavior may be due to the increase in the strength of adsorption process at higher temperatures, suggesting that chemisorption may be the type of adsorption of the inhibitor molecule on carbon steel surface. Thus, the predominance of corrosion inhibition for carbon steel using SFASS, suggests an appreciable contribution to the inhibition process via formation of Fe⁺²-SFASS complex on metal surface. These results were confirmed by FTIR, which will be discussed later

However, increasing the solution temperature leads to an increase in the current density values. Moreover slight cathodic shifts are observed in *E*_{corr} values at higher temperatures (not mentioned in the text). This result reflects enhancement of the cathodic hydrogen evolution reaction with temperature. Similar results obtained by Hassan [41] for corrosion inhibition of mild steel by triazole derivatives in HCl solution .The increase of corrosion rate is

pronounced with raise of temperature [42]. However, the values of $IE\%$ increase with temperature until reaching their plateau value at about 99.5% for SFASS at 100 ppm and 50 °C.

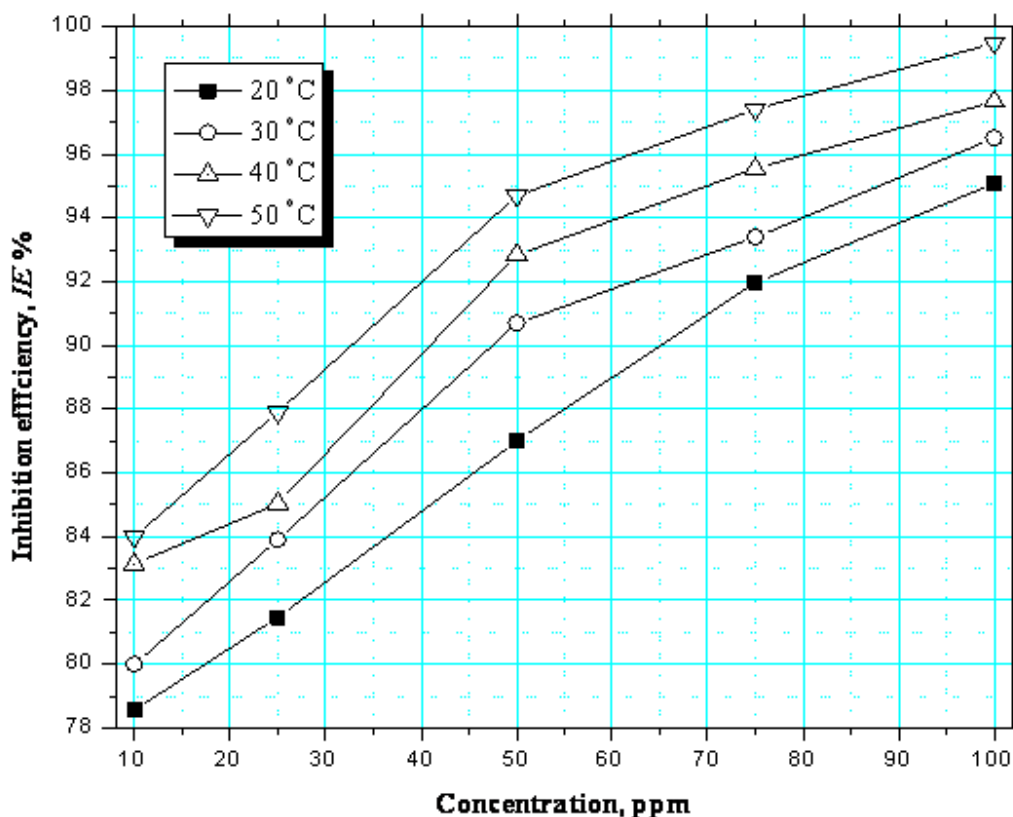


Fig. 7. Effect of various concentrations of SFASS on the inhibition efficiency of carbon steel in 1.0% NaCl saturated with CO₂ at different temperatures.

Arrhenius plots for carbon steel in the absence and presence of investigated inhibitor in 1% solution of NaCl saturated with CO₂ are shown in Fig. 8. The activation energy can be expressed by the Arrhenius equation:

$$\log I_{corr} = \log A - \frac{E_a}{2.33R T} \quad (4)$$

where T is the absolute temperature, A the constant and R universal gas constant.

The values of the apparent activation energy (E_a) of carbon steel corrosion determined from the slope of $\log I_{corr}$ vs. $1/T$ plots are given in Table 6. The activation energy decreases as SFASS concentration increases from 10-100 ppm. This can be explained as due to the enhancement of the inhibitor adsorption onto the metal surface at higher temperatures. Thus an increase in the surface coverage of carbon steel is expected. Similar results obtained by Hassan [41] for corrosion inhibition of mild steel by triazole derivatives in HCl solution. One can conclude that, the decrease in activation energy with increasing additive concentration, in addition to the increase in $IE\%$ in the presence of inhibitor with temperature, are suggestive of chemisorption of the inhibitor molecules on the metal surface [43].

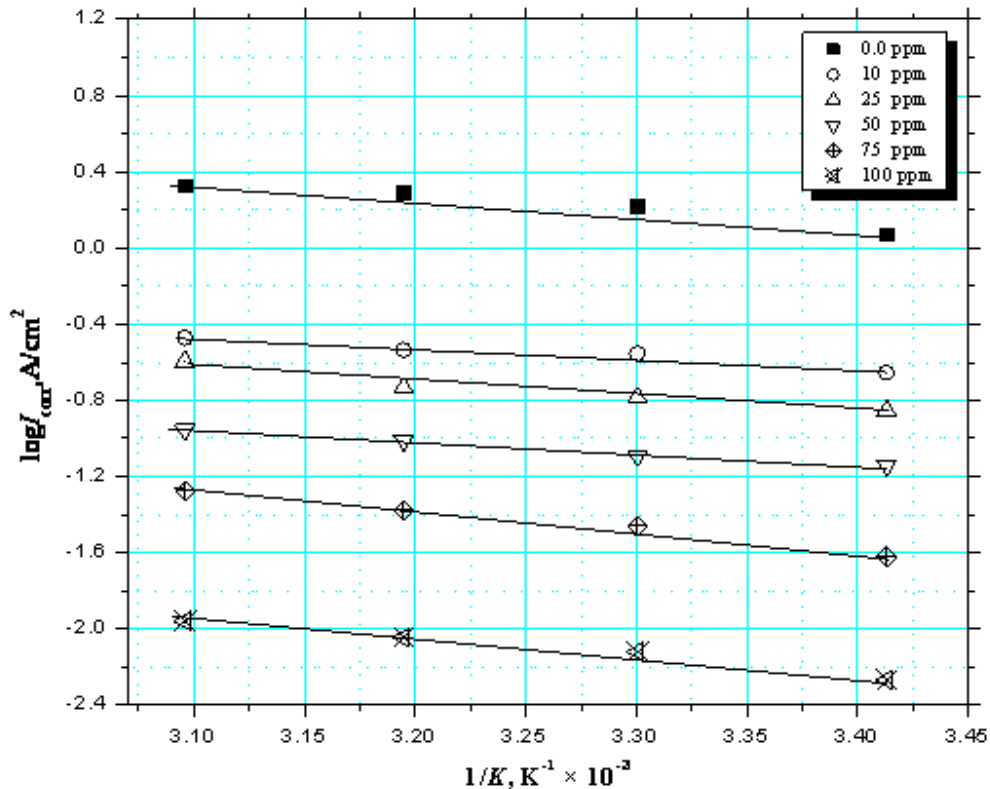


Fig. 8. Arrhenius plots for carbon steel corrosion in 1% NaCl solution saturated with CO₂ containing various concentrations of SFASS.

Table 6: Apparent activation energy in kJ/mol for carbon steel in 1%NaCl solution saturated with CO₂ containing various concentrations of SFASS

Concentration, ppm	<i>E_a</i> kJ/mol
0.0	6.651
10	4.406
25	4.151
50	3.925
75	3.811
100	3.724

3.5. Adsorption isotherms

The extent of corrosion inhibition depends on the surface conditions and mode of adsorption of inhibitor [44]. Assuming that the corrosion on the covered parts of the surface is equal to zero, so the corrosion takes place only on the uncovered parts of the surface, the degree of coverage (θ) was calculated from:

$$\theta = 1 - \frac{I_{inh.}}{I_{uninh.}} \tag{5}$$

where $I_{uninh.}$ and $I_{inh.}$ are the uninhibited and inhibited corrosion currents. In order to get more information about the mode of adsorption of the SFASS on the surface of carbon steel at different temperatures, the data obtained from cathodic and anodic Tafel polarization curves have been tested with several adsorption isotherms. Langmuir adsorption isotherm was found to fit well with the experimental data. The adsorption isotherm relationship of Langmuir is represented by the following equation:

$$\frac{C_i}{\theta} = \frac{1}{K_{ads.}} + C_i \tag{6}$$

where C_i is the concentration of the inhibitor and $K_{ads.}$ represents the adsorption equilibrium constant. Fitting curves of the polarization data to Langmuir adsorption isotherms for carbon steel in 1% NaCl solution saturated with CO_2 containing various concentrations of SFASS are shown in Fig. 9. It was found that, the values of K are relatively high and increase with increasing temperature. The relatively high value of the adsorption equilibrium constant reflects the high adsorption ability of this compound on the metal surface [45]. Accordingly this suggestion is confirmed that this inhibitor is chemisorption on the metal surface and the strength of adsorption increases with temperature.

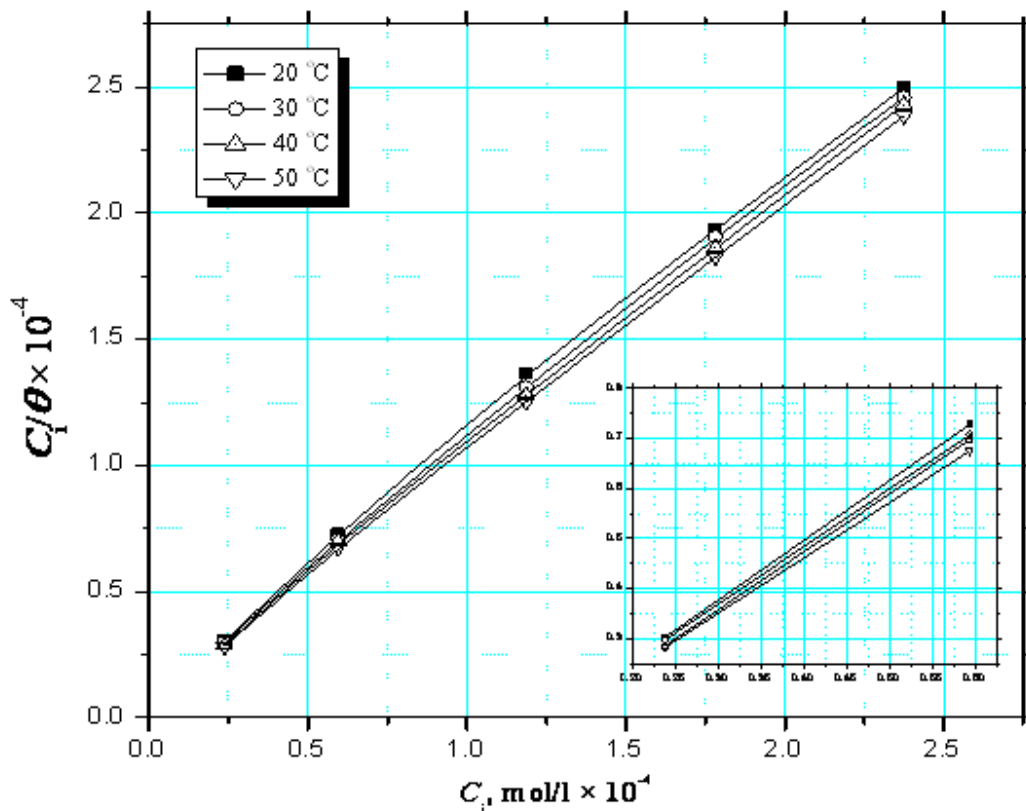


Fig. 9. Langmuir adsorption isotherm (C_i/θ vs. C_i) fitting of the obtained Tafel polarization data for carbon steel in 1.0 % solution of NaCl saturated with CO_2 containing various concentrations of SFASS inhibitor at different temperatures.

The average thermodynamic parameters ($\Delta H_{ads.}^o$, $\Delta S_{ads.}^o$ and $\Delta G_{ads.}^o$) for the inhibitor adsorption on the surface of carbon steel in the temperature range (20–50 °C) were determined from the slopes and intercept of the lines of $\ln K$ vs. $1/T$ plots (Fig. 10) according to the following equation [46]:

$$\ln K = \left(\frac{-\Delta H_{ads.}^o}{R} \cdot \frac{1}{T} \right) + \frac{\Delta S_{ads.}^o}{R} \tag{7}$$

where ΔH_{ads}^o and ΔS_{ads}^o are the enthalpy and entropy of the adsorption process, respectively. The calculated values of ΔH_{ads}^o , ΔS_{ads}^o and ΔG_{ads}^o . ($\Delta G_{ads}^o = \Delta H_{ads}^o - T\Delta S_{ads}^o$.) for carbon steel in 1% NaCl solution saturated with CO₂ containing various concentrations from SFASS are listed in Table 7. The value of ΔG_{ads}^o is high and negative suggesting that, the nature of the inhibitor adsorption on carbon steel surface is mainly chemisorption and spontaneous [47]. The negative value of ΔH_{ads}^o indicate that, the adsorption of inhibitor molecule is an exothermic process [48]. The magnitude of positive ΔS_{ads}^o and negative ΔH_{ads}^o values indicating that the occurrence of a replacement process during adsorption of inhibitor molecules on the carbon steel surface [47].

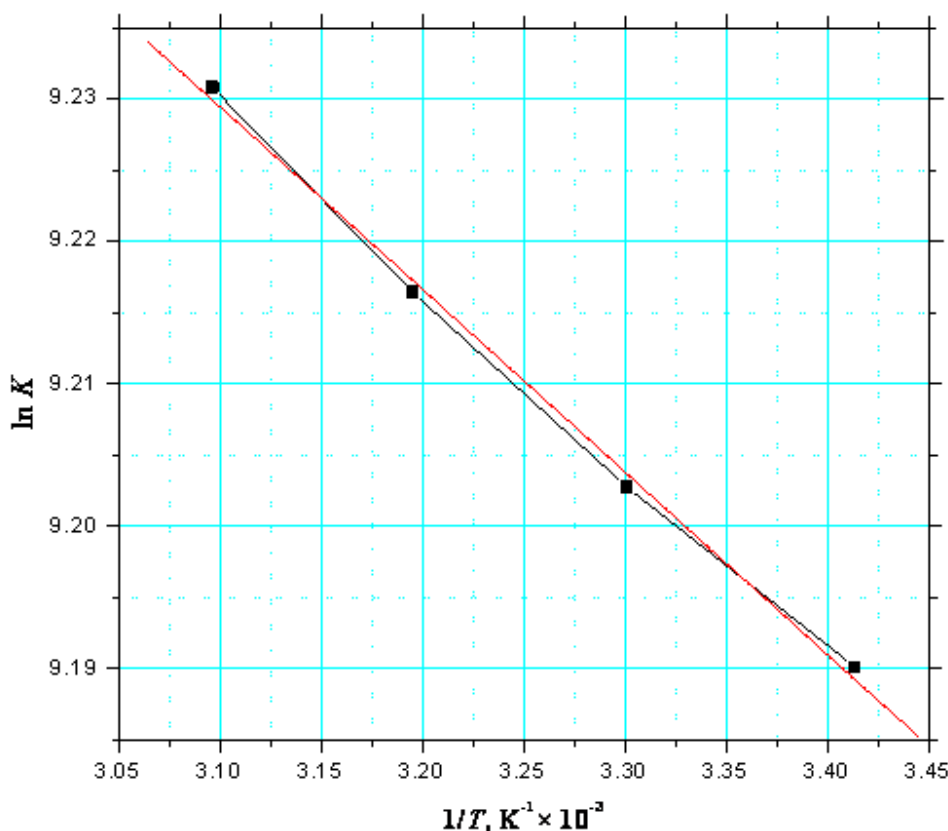


Fig. 10. Plotting of $\ln K$ vs. $1/T$ to calculate the thermodynamic functions for adsorption of SFASS on carbon steel surface in 1% NaCl solution saturated with CO₂.

Table 7: The thermodynamic parameters for SFASS adsorption on the surface of carbon steel in 1% NaCl solution saturated with CO₂

Parameters	$-\Delta G_{ads}^o$, (kJ/mol)	$-\Delta H_{ads}^o$, (kJ/mol)	ΔS_{ads}^o , (J/mol K)
Values	50.93	1.072	161

3.6. Analysis of the protective film by Fourier transform infrared spectroscopy (FTIR).

It has been established that FTIR spectrophotometer is a powerful instrument that can be used to determine the type of bonding for organic inhibitors absorbed on the metal surface. In present study, reflectance FTIR spectra were used to support the fact that corrosion inhibition of carbon steel in NaCl solution saturated with CO₂ is due to the adsorption of inhibitor molecules on the carbon steel surface. The FTIR spectrum of pure SFASS is given in Fig.

11(a). The C-H aliphatic stretching frequency is seen in the levels of 2950 and 2900 cm^{-1} . The peak at about 1690 cm^{-1} is due to the C=O. At the levels of 760 cm^{-1} , 780 cm^{-1} the stretching S–O and at the levels of 1350 cm^{-1} and 1335 cm^{-1} the S=O stretching frequency are observed. FTIR spectrum of a film layer formed on metal surface after dipping in the solution of 0.1% NaCl saturated with CO_2 containing 100 ppm SFASS for a period of four days is shown in Fig. 11(b). The S=O stretching frequency drops from the levels of 1350 cm^{-1} and 1335 cm^{-1} to the level of 1320 cm^{-1} (Fig. 11(b)). This suggests that electron cloud of S=O is shifted from S=O up to Fe^{2+} resulting in formation of Fe^{2+} -SFASS complex on metal surface [49].

Besides blockading wide surface, the sulfating group in SFASS molecule increases the adsorbability of surfactant on metal surface. That means a complex of Fe^{2+} -SFASS is formed as a result of bonding surfactant molecule by either electrons or free electron pairs on metal surface [49]. This known state as chemisorptions is also supported by the results of FTIR spectrum. Besides, while the polar head group was orientating towards metal surface due to surface-active feature of SFASS, the effect of inhibition increases by forming a hydrophobic barrier in the solutions containing aggressive ions like Cl [50]. Thus the surfactants create a hydrophobic barrier to aggressive ions.

From data in Fig. 11, it can be concluded that, the corrosion inhibition of carbon steel in NaCl solution by SFASS was due to the formation of the protective film from Fe^{2+} -SFASS complex.

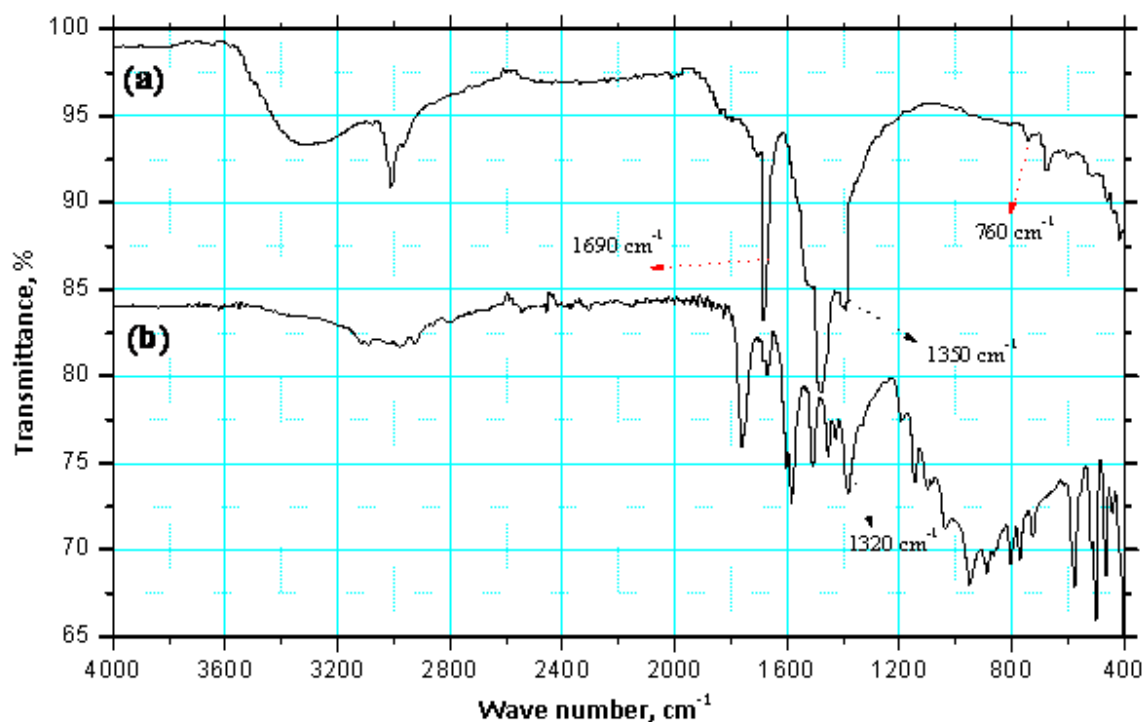


Fig. 11. FTIR spectra of pure SFASS and those of films formed on carbon steel after immersion in 1% NaCl solution saturated with CO_2 (a) pure SFASS (b) 1% NaCl solution saturated with CO_2 + 100 ppm SFASS.

3.7. Corrosion inhibition mechanism by surfactant molecule

The transition of metal/solution interface from a state of active dissolution to the passive state of great interest [51]. Adsorption of the surfactant molecules occurs because the interaction energy between the surfactant molecules and the metal surface is higher than that between water molecules and the metal surface. So the inhibition effect by surfactants is attributed to the adsorption of the surfactant molecule via their functional groups onto the metal surface. The adsorption rate is usually rapid and hence the reactive metal is shielded from the aggressive environment. Corrosion inhibition depends on the adsorption ability of the surfactant molecules on the corroding surface, which is directly related to the capacity of the surfactant to form clusters (micelles). The critical micelle concentration, CMC, is a key factor in determining the effectiveness of a corrosion

inhibitor. Below CMC as the surfactant concentration increases, the molecules tend to aggregate at the interface, and this interfacial aggregation reduces the surface tension. Above CMC the metal surface is covered with a monolayer of surfactant molecules and the additional molecules combine to form micelles or multiple layers. This, consequently, does not alter the surface tension and the corrosion rate [52].

CONCLUSION

The following conclusions can be drawn from this study:

1. The synthesized sulfated fatty acid sodium salt surfactant acts as an effective corrosion inhibitor for carbon steel in 1% NaCl solution saturated with CO₂.
2. The data obtained from all the used methods are in good agreement with each other. The inhibition efficiency increased as both concentration of the inhibitor and temperature are increased.
3. The inhibition efficiency (*IE* %) reached to 99.50% at 100 ppm of the inhibitor and at 50 °C.
4. SFASS acts as an inhibitor of mixed type of the carbon steel in NaCl solution.
5. The adsorption of synthesized surfactant on carbon steel surface obeyed Langmuir adsorption isotherm, and is chemically adsorbed on the metal surface.
6. The activation energy (*E_a*) decreases as SFASS concentration increases. This can be explained as due to the enhancement of the inhibitor adsorption onto carbon steel surface at higher temperatures.
7. The reflectance FTIR analysis showed that the inhibition of carbon steel corrosion occurred due to the formation of a protective film on the metal surface through adsorption of SFASS, and FTIR spectra reveal that the protective film consists of Fe²⁺-SFASS.
8. The critical micelle concentration, CMC, is a key factor in determining the effectiveness of a corrosion inhibitor.

REFERENCES

- [1] Ramesh Babu B, Thangavel K., *Method Mater.* **2005**, 52, 219–225.
- [2] Fouda AS, Mostafa HA, Heakal FE, Elewady GY, *Corros. Sci.*, **2005**, 47, 1988–2004.
- [3] Yurchenko R, Pogrebova L, Pilipenko T, Shubina T, *Russian J. Appl. Chem.*, **2006**, 79, 1100–1104.
- [4] Zhang ST, Tao ZH, Li WH, Hou BR, *Appl. Surf. Sci.* **2009**, 255, 6757–6763.
- [5] Li DG, Feng YR, Bai ZQ, Zheng MS, *Applied Surface Science*, **2007**, 253 (20), 8371–8376.
- [6] Li, T, Yang, Y, Gao, K, Lu, M., *Journal of University of Science and Technology Beijing, Mineral, Metallurgy, Material*, **2008**, 15 (6), 702–706.
- [7] Lopez DA, Simison SN, de Sanchez SR, *Corro. Sci.*, **2005**, 47 (3), 735–755.
- [8] Nescic S, Postlethwaite J, Olsen S, *Corrosion* **1996**, 52 (4), 280–294.
- [9] Sun W, Nescic S., *Corrosion*, **2008**, 64 (4), 334–346.
- [10] Sun W, Nescic S, Papavinasam S, *Corrosion*, **2008**, 64 (7), 586–599.
- [11] Wang F, Postlethwaite J, Modelling of Aqueous CO₂ Corrosion of Iron in Turbulent Pipe Flow, *CORROSION/2001*, paper no. 41 (Houston, TX: NACE, **2001**).
- [12] Bilkova K, Gulbrandsen E, *Electrochemical Acta*, **2008**, 53 (16), 5423–5433.
- [13] Dayalan E, de Moraes FD, Shadley JR, Shirazi A, Rybicki EF, CO₂ *CORROSION/1998*, paper no. 51 (Houston, TX: NACE, **1998**).
- [14] Chokshi K, Sun W, Nescic S, *CORROSION/2005*, (Houston, Texas: NACE, **2005**).
- [15] El-Etre AY, Abdallah M, *Corros. Sci.*, **2000**, 42, 731.
- [16] Abdallah M, *Corros. Sci.* **2002**, 44, 717.
- [17] Hosseini SMA, Azimi A, *Corros. Sci.*, **2009**, 51, 789.
- [18] El Maghraby AA, Soror TY, *Advances in Applied Science Research*, **2010**, 1 (2): 156–168
- [19] El Maghraby AA, Soror TY, *Advances in Applied Science Research*, **2010**, 1 (2): 143–155.
- [20] Fuchs-Godec R, *Colloids Surf. A.*, **2006**, 280, 130–139.
- [21] Fuchs-Godec R, Doleček V, *Colloids Surf. A.*, **2004**, 244, 73–76.
- [22] Fuchs-Godec R, *Acta Chim. Slov.*, **2007**, 54, 492–502.
- [23] Fuchs-Godec R, *Electrochim. Acta.*, **2007** 52, 4974–4981.
- [24] Fuchs-Godec R, *Electrochim. Acta.*, **2009**, 54, 2171–2179.
- [25] Fuchs-Godec R, *Ind. eng. chem. res.*, **2010**, 49, 6407–6415.
- [26] Negm NA, Zaki FM, *Colloids Surf. A.*, **2008**, 322, 97–102.
- [27] Li X, Deng S, Mu G, Fu H, Yang F, *Corros. Sci.*, **2008**, 50, 420–430.

- [28] Hegazy MA, Zaky MF, *Corros. Sci.*, **2010**, 52, 1333-1341.
- [29] Afanas'ev BN, Akulova YP, Polozhentseva YA, *Protection of Metals*, **2008**, 44 (2), 134–140.
- [30] El-Sayed A, Mohran HS, Abd El-Lateef HM, *Journal of Power Sources*, **2010**, 195, 6924–6936.
- [31] Zhao T, Mu G, *Corros. Sci.*, **1997**, 41, 1937.
- [32] Singh A, Singh VK, Quraishi M.A, *Rasayan J. Chem.*, **2010**, 3 (4), 811-824.
- [33] Yan Y, Weihua L, Lankun Cai, Baorong Hou, *Electrochimica Acta* , **2008**, 53, 5953–5960.
- [34] Miller CA, Qutubuddin , Eike HF, Parfitt CD (Eds), *Interfacial Phenomena in polar Media*, 'Surfactant Science Series', Vol. 21, (Marcel Dekker, Inc., New York **1987**), 166.
- [35] Rosen MJ, in 'Surfactants and Interfacial Phenomena', (Wiley, New York, **1978**), pp. 1–301.
- [36] El-Sayed A, Mohran HS, Abd El-Lateef HM, *Journal of Power Sources* , **2011**, 196, 6573–6582.
- [37] Tremont R, De Jesus-Cardona H, Garcia-Orozco J, Castro RJ, Cabrera CR, *J. Appl. Electrochem.*, **2000**, 30, 737.
- [38] Schultze JW, Wippermann K, *Electrochim. Acta*, **1987**, 32, 823.
- [39] Abdel Aal MS, Abdel Wahab AA, El-Sayed A, *Corrosion*, **1981**, 37, 557.
- [40] El-Sayed A, Shaker AM, Abd El-Lateef HM, *Corros. Sci.*, **2010**, 52, 72.
- [41] Hassan HH, *Electrochim. Acta*, **2007**, 53, 1722.
- [42] Amin MA, Abd El-Rehim SS, El-Sherbini EEF, Bayomi RS, *Electrochim. Acta*, **2007**, 52, 3588.
- [43] Sankarapapavinasam S, Ahmed FM, *J. Appl. Electrochem.*, **1992**, 22, 390.
- [44] Migahed MA, Azzam EMS, Al-Sabagh AM, *Materials Chemistry and Physics*, **2004**, 85, 273–279.
- [45] Sobramanyam NC, Mayannu SM, *J. Electrochem. Soc. India*, **1984**, 33, 273.
- [46] Frumkin AN, *Z. Phys. Chem.* **1915**, 116, 166.
- [47] El-Sayed A, *J. Appl. Electrochem.*, **1997**, 27, 193.
- [48] Abdel Nabey BA, Khamis E, Ramadan MS, El-Gindy A, in: 8th European Symp. Corros. Inhibitors, *Ann. Univi. Ferrara N.S. Sez.*, **1995**, 10, 299.
- [49] Zor S , Yazıcı B, Erbil M, *Corrosion Science*, **2005**, 47, 2700–2710.
- [50] Shalaby MN, Osman MM, El Key AA, *Anti-Corr. Methods Mat.*, **1999**, 46, 254.
- [51] Malik MA , Hashim MA, F. Nabi , AL-Thabaiti SA , Khan Z, *Int. J. Electrochem. Sci.*, **2011**, 6, 1927 – 1948.
- [52] Migahed MA, Abd-El-Raouf M, Al-Sabagh AM, Abd-El-Bary HM, *Electrochimica Acta*, **2005**, 50, 4683–4689.